Monthly Notices of the ROYAL ASTRONOMICAL SOCIETY

MNRAS **482,** 3109–3115 (2019)
Advance Access publication 2018 October 27

doi:10.1093/mnras/sty2909

A fast radio burst with a low dispersion measure

E. Petroff,[1,2,3★†] L. C. Oostrum,[1,2] B. W. Stappers,[4] M. Bailes,[2,5,6] E. D. Barr,[7] S. Bates,[4] S. Bhandari,[8] N. D. R. Bhat,[5,9] M. Burgay,[10] S. Burke-Spolaor,[11,12] A. D. Cameron,[3] D. J. Champion,[7] R. P. Eatough,[7] C. M. L. Flynn,[2] A. Jameson,[2,5] S. Johnston,[8] E. F. Keane,[13] M. J. Keith,[4] M. Kramer,[4,7] L. Levin,[4] V. Morello,[4] C. Ng,[14] A. Possenti,[10,15] V. Ravi,[16] W. van Straten,[17] D. Thornton[4] and C. Tiburzi[7]

Affiliations are listed at the end of the paper

Accepted 2018 October 24. Received 2018 October 24; in original form 2018 July 31

Downloaded from https://academic.oup.com/mnras/article-abstract/482/3/3109/5145856 by California Institute of Technology user on 10 April 2019

ABSTRACT

Fast radio bursts (FRBs) are millisecond pulses of radio emission of seemingly extragalactic origin. More than 50 FRBs have now been detected, with only one seen to repeat. Here we present a new FRB discovery, FRB 110214, which was detected in the high-latitude portion of the High Time Resolution Universe South survey at the Parkes telescope. FRB 110214 has one of the lowest dispersion measures of any known FRB (DM $= 168.8 \pm 0.5$ pc cm^{-3}), and was detected in two beams of the Parkes multibeam receiver. A triangulation of the burst origin on the sky identified three possible regions in the beam pattern where it may have originated, all in sidelobes of the primary detection beam. Depending on the true location of the burst the intrinsic fluence is estimated to fall in the range of 50–2000 Jy ms, making FRB 110214 one of the highest fluence FRBs detected with the Parkes telescope. No repeating pulses were seen in almost 100 h of follow-up observations with the Parkes telescope down to a limiting fluence of 0.3 Jy ms for a 2 ms pulse. Similar low DM, ultrabright FRBs may be detected in telescope sidelobes in the future, making careful modelling of multibeam instrument beam patterns of utmost importance for upcoming FRB surveys.

Key words: methods: data analysis – galaxies: statistics – radio continuum: transients.

1 INTRODUCTION

Fast radio bursts (FRBs) are observed as bright, millisecond radio transients of unknown origin (e.g. Lorimer et al. 2007; Thornton et al. 2013). FRBs are characterized by a high dispersion measure (DM) relative to the expected contribution due to the Galaxy, corresponding to a large electron column density along the line of sight. The entire population of more than 50 FRBs observed to-date 1 (Petroff et al. 2016) are believed to be extragalactic in origin. However, only one FRB source, FRB 121102, has been definitively localized to a host galaxy – a dwarf galaxy at $z = 0.19273(8)$ (Spitler et al. 2014; Chatterjee et al. 2017; Tendulkar et al. 2017).

Due to their short durations ($\lesssim$50 ms), high flux densities ($\gtrsim$1 Jy), and high inferred brightness temperatures ($\gtrsim 10^{36}$ K), progenitor models involving beamed emission from compact objects are often invoked to explain FRBs. Favoured models include young, millisecond magnetars in dense progenitor environments (Metzger, Berger & Margalit 2017), young pulsars in nearby galaxies (Connor, Sievers & Pen 2016; Cordes & Wasserman 2016), collapses of neutron stars to black holes (Falcke & Rezzolla 2014), binary neutron star mergers (Totani 2013), and energetic magnetars orbiting black holes (Michilli et al. 2018). However, current observations are insufficient to trace FRBs back to any of these progenitor scenarios with confidence. Ultimately, more well-localized sources with precise measurements of intrinsic flux (i.e. not convolved with an uncertain location in a telescope beam) and distance are needed to constrain theoretical models.

Shannon et al. (2018) and Macquart et al. (2018) have recently increased the FRB population by 22 sources from a large sample detected at the Australian Square Kilometre Array Pathfinder (ASKAP). These bursts, detected in a fly's eye survey occupy a lower DM and higher fluence range than the sample from more sensitive telescopes with DMs from 114 to 991 pc cm^{-3} and measured fluences from 34–420 Jy ms. If the FRB source count distribution is steep, these ultrabright events are expected to occur at a lower rate

★ E-mail: ebpetroff@gmail.com
† Veni Fellow.

[1] All published FRBs are available on the FRB Catalogue; http://www.frbcat.org

© 2018 The Author(s)
Published by Oxford University Press on behalf of the Royal Astronomical Society

than the lower fluence events typically detected by telescopes such as Parkes.

Here we present a new FRB detected with the Parkes 64 m telescope in the High Time Resolution Universe (HTRU) South survey in 2011, FRB 110214. This FRB has one of the lowest measured FRB DMs to-date and was detected in the sidelobes of two outer beams of the Parkes multibeam receiver, implying a high intrinsic peak flux density. In Section 2.1 we describe the observing system, in Section 2.2 we present the burst properties, in Section 3 we detail our efforts to localize FRB 110214 within the Parkes beam pattern, in Section 4 we present results of follow-up at the possible locations of the FRB including searches for repeating pulses (Section 4.1) and attempts to identify a host galaxy (Section 4.2), and in Section 5 we summarize these results and how they relate to the broader population of FRBs.

2 OBSERVATIONS

2.1 Setup

The discovery observations of FRB 110214 were part of the HTRU South survey conducted at the Parkes radio telescope in New South Wales, Australia (Keith et al. 2010) using the Parkes multibeam receiver (hereafter MBl; Staveley-Smith et al. 1996). The MB has 13 circular feed horns, each of which forms an elliptical beam on the sky with a full width at half-maximum (FWHM) of approximately 14′.4. For the HTRU survey, each beam has a separate data stream through the Berkeley Parkes Swinburne Recorder (BPSR) which records 2 bit data to disc in the form of 1024 frequency channels across 400 MHz of bandwidth from 1.182 to 1.582 GHz with 64µs time sampling (Keith et al. 2010). Only 340 MHz of the total bandwidth is used as the top 60 MHz of the band is highly contaminated with radio frequency interference (RFI) from satellites.

The HTRU South survey data were collected between 2008 and 2014 and consisted of three survey regions at low, intermediate, and high Galactic latitudes with integration times of 4300, 540, and 270 s, respectively. The HTRU high-latitude data were partially processed by Thornton et al. (2013) leading to the discovery of FRBs 110220, 110626, 110723, and 120127. A full re-processing of the high-latitude survey was done to search for FRBs using the HEIMDALL single pulse search software[2] for events that match the criteria of an FRB outlined in previous publications (Petroff et al. 2015; Champion et al. 2016; Bhandari et al. 2018).

In this processing all four FRBs detected by Thornton et al. (2013) were recovered as well as six others. Five new detections were reported in Champion et al. (2016): FRBs 090625, 121002, 130626, 130628, and 130729. A small fraction of the high-latitude data, approximately 0.5 per cent, were not processed at the time of the Champion et al. paper due to processing failures on the gSTAR supercomputer. In re-processing these failed jobs, a new FRB was discovered. We describe the sixth detection in the following section.

2.2 FRB 110214

The fast radio burst FRB 110214 was recorded at the Parkes telescope during an observation of the high-latitude portion of the HTRU South survey. The burst occurred at 2011-02-14 07:14:10.353 UTC at a reference frequency of 1.382 GHz, the middle of the observing band. In an initial search with HEIMDALL, the burst was found in only a single beam (Beam 2) with $S/N_{beam2} = 13$, $\Delta t = 1.9(9)$ ms, and DM $= 168.8(5)$ pc cm^{-3}, one of the lowest DMs for an FRB reported thus far. The beam was centred at RA = 01:21:17 Dec. = −49:47:11 corresponding to a Galactic latitude and longitude $(\ell, b) = (290.^{\circ}7, -66.^{\circ}6)$. For a full description of the burst properties, see Table 1.

Despite its proximity in time to other HTRU detections, having occurred only 6 d before FRB 110220, FRB 110214 was missed in previous searches. We attribute this to human error and the novelty of the field of FRBs at the time of the first search of the data. At the time these data were being searched by Thornton et al. the observational characteristics of FRBs were poorly classified and a low-signal-to-noise ratio (S/N), low DM candidate present in only half of the observing band (see Fig. 1) may have been rejected as spurious. The DM excess of FRB 110214 is still high relative to the expected DM contribution of the Galaxy along the line of sight: 31 and 21 pc cm^{-3} according to the NE2001 and YMW16 models, respectively (Cordes & Lazio 2002; Yao, Manchester & Wang 2017). However, the burst was ultimately discovered in the reprocessing of the entire survey undertaken for Champion et al. (2016) at which point it was investigated further. In deeper searches of the other beams of the MB, FRB 110214 was also found to be weakly detected in Beam 8, with $S/N_{beam8} = 6$ (see Fig. 1) and was not detected above a threshold of $S/N \geq 5$ in any other beams.

The spectral index of the burst in both detection beams is negative, with significantly more signal in the lower half of the band. Integrating over the bottom 50 per cent of the Parkes bandwidth, from 1.182 to 1.352 GHz, results in a higher significance detection in both beams with $S/N_{beam2\_lower} = 17$ and $S/N_{beam8\_lower} = 7$ (see Table 2) and non-detections in all other beams. The data for this observation are not bandpass corrected; BPSR sets the levels for an observation using the first 10 s of data. However, the BPSR bandpass shapes are consistent across many observations and close to flat.

Table 1. Observed and derived properties of FRB 110214. The ranges for the peak flux and fluence of the burst are given here as derived properties due to the highly off-axis burst location and are based on the estimated origin of the FRB in the MB beam pattern; see text for further details. Derived values for redshift and distance are based on the estimated relation between DM and redshift of $z \sim DM_{excess}/1000$ (Ioka 2003).

Observed properties	
Event date UTC	2011 Feb 14
Event time UTC, $\nu_{1.382\,GHz}$	07:14:10.353
Event time, ν_{∞}	07:14:09.986
Beam 2 RA	01:21:17
Dec.	−49:47:11
Beam 8 RA	01:19:07
Dec.	−49:26:40
Beam 2 (ℓ, b)	(290.7°, −66.6°)
Beam full width at half-maximum	14.4 arcmin
DM_{FRB} (pc cm^{-3})	168.8(5)
Detection S/N_{beam2}	13(1)
Detection S/N_{beam8}	6(1)
Observed width, Δt (ms)	1.9(9)
Derived properties	
Peak flux density, $S_{\nu,\,1200\,MHz}$ (Jy)	27–1055
Fluence, $\mathcal{F}$ (Jy ms)	54–2057
$DM_{MW,\,NE2001}$ (pc cm^{-3})	31.1
$DM_{MW,\,YMW16}$ (pc cm^{-3})	21.0
Redshift, z	<0.14
Comoving distance (Mpc)	462
Luminosity distance (Mpc)	513

[2] https://sourceforge.net/projects/heimdall-astro/

Downloaded from https://academic.oup.com/mnras/article-abstract/482/3/3109/5145856 by California Institute of Technology user on 10 April 2019

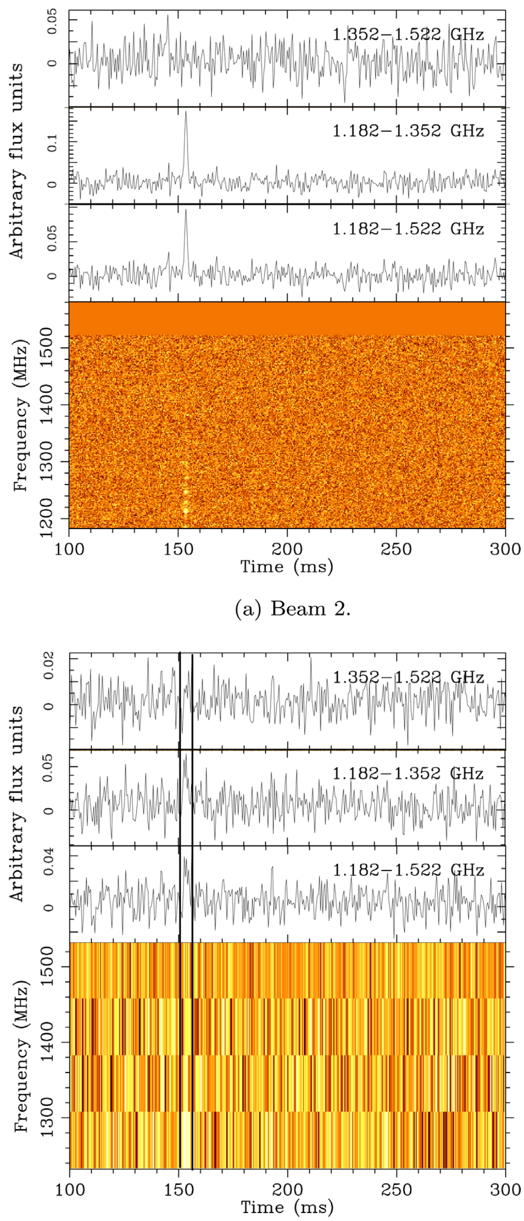

(a) Beam 2.

(b) Beam 8.

Figure 1. The dynamic spectra of FRB 110214 detected in (a) Beam 2 and (b) Beam 8 of the Parkes multibeam receiver. The effects of dispersion have been removed and the integrated timeseries are shown for each beam over the top half (top), the bottom half (middle), and the entire range (bottom) of the bandwidth. The frequency channels between 1522 and 1582 MHz have been masked in both beams due to persistent RFI. For Beam 8, the frequency time spectrum has been integrated into four frequency channels and the pulse range is bordered by vertical lines to guide the eye.

Table 2. The S/N of FRB 110214 in the primary (Beam 2) and secondary (Beam 8) detection beams in different sub-bands. The burst was not detected in the top sub-band of either beam.

	S/N		
	1.352–1.522 GHz	1.182–1.352 GHz	Full band
Beam 2	<5	17.0	13.4
Beam 8	<5	7.0	6.0

While the pulse may have an intrinsically negative spectral index either due to its emission process or Galactic scintillation, the detection of the burst in multiple beams of the receiver and stronger detections at lower frequencies leads to the conclusion that the source location might be far off-axis relative to both beams (>7 arcmin). Given the significantly reduced sensitivity of the telescope at off-axis positions, the intrinsic flux density of FRB 110214 must be high.

3 LOCALIZATION OF FRB 110214

To estimate the location of FRB 110214 in the beam pattern of the MB, the beam model developed for FRB 150807 by Ravi et al. (2016) was modified to reflect the case of this particular burst. Briefly, the model consists of radiation patterns for each individual beam of the MB accounting for the geometry of the dish and receiver, blockage from the focus cabin, and edge tapering for each beam calculated at each point on a 1000 × 1000 pixel rectangular grid covering an area of 3 deg^2 centred on the central beam. Ravi et al. found this model closely approximated the observed response of the central, inner, and outer beams of the MB for bright Galactic pulsars. While any analytic model may be insufficient for the purposes of precisely pinpointing a location of the FRB on the sky, in the case of the MB it is the best approximation possible since the actual beam pattern is not fully mapped with real measurements. Nonetheless, it can provide useful information about the high-probability region(s) where the burst may have originated and how bright it may have been intrinsically.

Due to the non-detection of FRB 110214 at higher frequencies (see Table 2) only the lower half of the BPSR frequency bandwidth was used in the localization analysis. The beam pattern model from Ravi et al. was modified to only model the MB response in the range 1.182–1.352 GHz. Using a method similar to that described in Obrocka, Stappers & Wilkinson (2015), the beam pattern model was searched for regions where the ratio between the signal strength in beams 2 and 8 matched that of the detected pulse in the Parkes data and accounting for the different gains in each beam. In the 170 MHz frequency band used, this corresponds to a ratio $\left(\mathrm{S/N_{beam2\_lower}}\right) / \left(\mathrm{S/N_{beam8\_lower}}\right) = \mathrm{S/N_{2:8}} \sim 2.5$. Assuming an error of ±1 on the detection S/N of each beam provides a window of allowable ratios $2.125 \lesssim \mathrm{S/N_{2:\,8}} \lesssim 2.93$ between beams 2 and 8. Further constraints are placed by the non-detection of the pulse in any other beams with a threshold of S/N > 5, such that $\mathrm{S/N}_{2:\,i} <$ 17.0/5.0 for all beams i except Beam 2 and Beam 8.

Within these constraints, three allowed regions in the beam pattern emerge,[3] as shown in Fig. 2. The three regions vary in distance from the primary detection beam; Region A is the closest, placing FRB 110214 in the first sidelobe of Beam 2. Region B is elongated away from the detection beams and lies along a line of constant $\mathrm{S/N_{2:\,8}}$ in the outer sidelobes. Region C is approximately 30 arcmin away from the primary detection beam and would place FRB 110214 in an outer sidelobe of the MB beams.

For each region, we estimate the intrinsic flux density and fluence of FRB 110214 required to produce the observed signal in the data. We calculate the intrinsic peak flux density of FRB 110214 if it were located in each region. In each case we calculate an average and median peak flux density for each region, as estimated flux density increases rapidly with distance from the centre of the primary beam

[3]Contours of the localization regions are provided in a supplementary file of this manuscript.

Downloaded from https://academic.oup.com/mnras/article-abstract/482/3/3109/5145856 by California Institute of Technology user on 10 April 2019

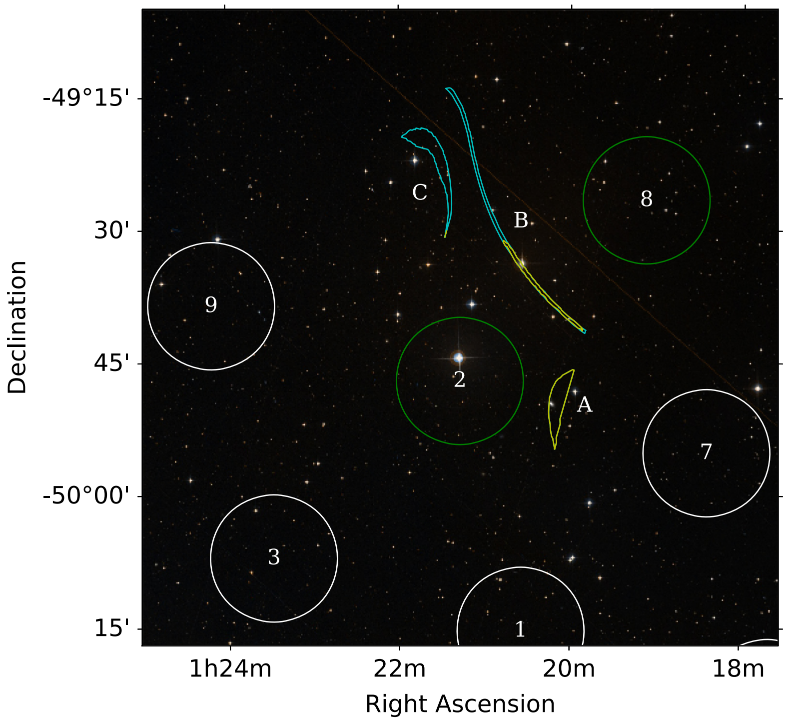

Figure 2. The beams of the MB and the three 1σ localization regions identified for FRB 110214 using the model from Ravi et al. (2016) over the frequency range 1.182–1.352 GHz. The radio regions are overlaid on a sky image from the Sloan Digital Sky Survey (SDSS; York et al. 2000). The regions (labelled A, B, and C) correspond to locations that produce the detected S/Ns of FRB 110214 in beams 2 and 8 (green), with non-detections in all other beams (white). The combined area of the 1σ regions is roughly 52 arcmin^2. Assuming a Euclidean source count distribution for the FRB population, regions with a relative likelihood $\geq$10 per cent of the minimum flux are also shown for Regions B and C (yellow). Region A remains unchanged (see text).

Table 3. Estimated intrinsic peak flux density S and fluence $\mathcal{F}$ of FRB 110214 for an origin in each of the localization regions identified in the beam pattern. Flux density and fluence are calculated using data in the frequency range 1.182–1.352 GHz. In each case an average (avg) and median (med) value for flux density and fluence is given.

Region	$S_{\rm avg}$ (Jy)	$\mathcal{F}_{\rm avg}$ (Jy ms)	$S_{\rm med}$ (Jy)	$\mathcal{F}_{\rm med}$ (Jy ms)
A	28.5	55	27.8	54
B	504	982	110	215
C	899	1754	1055	2057

and can significantly affect the average for an elongated region. We calculate a fluence $\mathcal{F} = S \times \Delta t$ where we use the observed pulse width $\Delta t = 1.95$ ms since no substantial broadening of the pulse is expected in the case of an off-axis detection. The estimated flux densities and fluences for these regions are summarized in Table 3.

3.1 Region A

Region A occupies an area of $\sim$10 arcmin^2 (1σ) centred at RA 01:20:09 Dec. –49:49:37 (11 arcmin from Beam 2 centre). If FRB 110214 originated in or near this region we estimate an intrinsic peak flux density of $S_{\rm A,avg} \approx 29$ Jy or $S_{\rm A,med} \approx 28$ Jy. These two estimates are close due to the compactness of the region and its proximity relative to the primary detection beam. These values correspond to estimated FRB fluences of $\mathcal{F}_{\rm A,avg} \approx 55$ Jy ms and $\mathcal{F}_{\rm A,med} \approx 54$ Jy ms. The full range of fluence values in Region A is 34–95 Jy ms.

3.2 Region B

Region B is narrow and elongated with a total area of $\sim$14 arcmin^2 (1σ) extending from RA 01:19:48 Dec. –49:41:31 at its closest to the primary beam (15 arcmin from Beam 2 centre) to RA 01:21:25 Dec. –49:14:13 at its furthest (33 arcmin from Beam 2 centre). In this region the estimated peak flux density for FRB 110214 is $S_{\rm B,avg} \approx 504$ Jy and $S_{\rm B,med} \approx 110$ Jy. These values, in turn, correspond to estimated fluences for FRB 110214 of $\mathcal{F}_{\rm B,avg} \approx 982$ Jy ms and $\mathcal{F}_{\rm B,med} \approx 215$ Jy ms. The full range of fluence values in Region B is 72–8472 Jy ms.

3.3 Region C

Region C has a large area of $\sim$28 arcmin^2 (1σ). While also highly elongated, the region is approximately centred at RA 01:21:36 Dec. –49:17:34 (30 arcmin from Beam 2 centre). An FRB with the observed parameters of FRB 110214 originating from this region would have an intrinsic flux $S_{\rm C,avg} \approx 899$ Jy or $S_{\rm C,med} \approx 1055$ Jy. This corresponds to a fluence of $\mathcal{F}_{\rm C,avg} \approx 1754$ or $\mathcal{F}_{\rm C,med} \approx 2057$ Jy ms. The full range of fluence values in Region C is 127–2996 Jy ms.

3.4 Spectral properties

The presence of three regions here is not particularly surprising. The detection significance of FRB 110214 is much lower than in the case of other multibeam FRBs such as FRB 010724 and FRB 150807 (Lorimer et al. 2007; Ravi et al. 2016), making the triangulation of the burst location on the sky more challenging. In the cases of FRB 010724 and FRB 150807 an additional localization constraint

Downloaded from https://academic.oup.com/mnras/article-abstract/482/3/3109/5145856 by California Institute of Technology user on 10 April 2019

could be made using multiple sub-bands. No regions were identified in the beam pattern matching the constraints outlined in Section 3 that also satisfied the condition of non-detection in the top half of the band assuming a flat spectrum. Thus the FRB itself must have a negative spectral index either due to intrinsic emission or propagation effects along the line of sight. Only weak constraints on the spectral index or localization can be derived due to the complete lack of signal at these frequencies. All calculations for the intrinsic peak flux density and fluence of FRB 110214, therefore, only consider emission over 50 per cent of the Parkes observing band, as this is where signal was present for analysis.

4 FOLLOW-UP OBSERVATIONS

4.1 Search for repeating pulses

Given the low DM and the large implied fluence of 50–2000 Jy ms for FRB 110214, significant time was spent on follow-up to search for repeating pulses. Repeating pulses from FRB 121102 are several orders of magnitude fainter in peak flux density (Spitler et al. 2016; Chatterjee et al. 2017), but the distance to the host galaxy of the repeating FRB is almost twice that of the estimated distance to FRB 110214 (Tendulkar et al. 2017). The burst was identified in the HTRU data in 2016 February. Due to the commissioning of the Effelsberg phased array feed (PAF; Chippendale et al. 2016) at the time, the only available receiver at the Parkes focus was the single pixel H–OH receiver.[4] The H–OH receiver was used over a 256 MHz bandwidth centred at 1.386 GHz with a beam FWHM of 14.′8. A total of 62.5 h of follow-up were conducted with the H–OH receiver with 96µs time resolution centred at the position RA 01:20:13 Dec. –49:49:47, in Region A. No single pulses were found at any DM $\leq$ 5000 pc cm^{-3} above S/N $>$ 5 over the entire bandwidth, corresponding to a flux density threshold of 0.15 Jy for a 2 ms pulse. These data were heavily affected by RFI since no multibeam coincidence could be used for candidate rejection and we estimate that approximately 5 per cent of the data were ruined by interference. This estimate is derived from the total number of time samples which had to be masked due to the presence of impulsive broad-band RFI across all observations.

The early choice to focus on Region A was motivated by a limited amount of telescope time, the availability of only a single-pixel receiver, and the presence of a bright nearby galaxy in the region (Section 4.2). An origin in Region A would also imply the lowest intrinsic flux density of $17 > S_{\rm peak} > 49$ Jy, thought to be the most likely as ultrabright FRBs such as FRB 010724 (800 $\pm$ 400 Jy; Ravi 2019), FRB 170827 (50 Jy; Farah et al. 2018), and FRB 180309 ($>$20 Jy; Oslowski et al. 2018) were not as common, nor were the high fluence ASKAP FRBs known.

In 2016 December the MB was re-installed in the Parkes focus cabin and additional follow-up efforts were undertaken. An additional 32.7 h of follow-up were conducted with the MB with the central beam centred on Region A such that outer beams covered the majority of Regions B and C. These data were searched with HEIMDALL for pulses matching the same criteria as above and no pulses were found at any DM above S/N $>$ 5 over the entire bandwidth, corresponding to a flux density threshold of 0.13 Jy for a 2 ms pulse.

[4]https://www.parkes.atnf.csiro.au/observing/documentation/ user_guide/pks_ug_3.html#Receiver-Fleet

4.2 Identifying a host galaxy

Each region was matched to several catalogues with the aim of identifying a possible host galaxy. No sources were found in the Chandra Source Catalogue or the *XMM–Newton* Serendipitous Source Catalogue (Evans et al. 2010; Rosen et al. 2016). The near-infrared Vista Hemisphere Survey (VHS; McMahon et al. 2013) only covers region C and two thirds of region B, however it already identifies about 250 objects as possible galaxies in those regions. As redshifts are not available for these sources, we are unable to reduce this number by considering the maximum expected redshift of the FRB.

All regions are fully covered by the 2 micron All-Sky Survey (2MASS; Skrutskie et al. 2006). It reports one known galaxy in region A at RA 01:20:13.411 Dec. –49:49:47.64. This galaxy, FRL 692, is an elliptical galaxy at a redshift of $z \approx 0.025$ (Fairall 1984). At this redshift, the intergalactic medium (IGM) is expected to contribute $\sim$ 17–25 pc cm^{-3} to the total DM from the Yao et al. (2017) and Ioka (2003) models, respectively. The total DM in the host galaxy (i.e. the excess from the Galaxy and the IGM) would then be 131 pc cm^{-3} using YMW16 and 113 pc cm^{-3} using NE2001 and the IGM model from Ioka (2003). We do not expect a significant contribution to the DM due to an interstellar component in elliptical galaxies (Xu & Han 2015); however, if the source of the FRB were embedded in an ionized progenitor region like FRB 121102, such a host contribution could be feasible.

Considering the possibility that the host of FRB 110214 is similar to that of FRB 121102, we estimate the total number of possible host galaxies assuming the host to be a dwarf galaxy at least as massive as the host galaxy of FRB 121102 [$(4-7) \times 10^7$ M$_\odot$; Tendulkar et al. 2017]. The number density of galaxies can be described by the Schechter function

$$\Phi(M)\,{\rm d}M = \phi_*\,(M/M_*)^\alpha\,{\rm e}^{M/M_*}\,{\rm d}M, \tag{1}$$

where $\Phi(M)$ is the number density of galaxies per unit mass, M_* is the characteristic mass, and ϕ_* is a normalization constant. We consider two mass functions: (1) the stellar mass function for blue galaxies (defined as $u - r \lesssim 1.9$; Baldry et al. 2012), which should more closely resemble the repeater host galaxy as they have a higher specific star formation rate than red galaxies, and (2) the H I mass function (Haynes et al. 2011), which is likely more complete for dwarf galaxies as they tend to have relatively high H I to stellar mass ratios $(1-10)$, making them easier to detect in H I. Integrating these mass functions from $M_{\rm stellar} = 4 \times 10^7$ M$_\odot$ to the maximum mass considered to be a dwarf galaxy, 10^{10} M$_\odot$, and allowing the H I to stellar mass ratio to vary between 1 and 10, gives a dwarf galaxy number density of $n = (0.02-0.06)\,{\rm Mpc}^{-3}$.

Assuming the mass function and galaxies do not evolve significantly between $z = 0$ and 0.14, which is reasonable given the low redshift, the total expected number of dwarf galaxies in the FRB 110214 error region is simply $n\,V_{\rm C}$, where $V_{\rm C}$ is the comoving volume, which we calculate from the redshift assuming the best-fitting cosmological parameters of Planck Collaboration et al. (2016). The number of dwarf galaxies as a function of redshift is shown in Fig. 3. We also show the expected number of massive $M_{\rm stellar} > 10^{11}$ M$_\odot$ galaxies, based on the luminosity function of blue galaxies of Faber et al. (2007), from which we find a number density of $n = (1.5-2.0) \times 10^{-3}\,{\rm Mpc}^{-3}$. For a host DM contribution of zero, between 5 and 20 dwarf galaxies are expected within the total volume of all three regions. In contrast, no massive galaxies are expected at all. Hence, the proximity of FRL 692 is unlikely, but without more precise localization of the FRB we cannot say anything about an association with certainty.

Downloaded from https://academic.oup.com/mnras/article-abstract/482/3/3109/5145856 by California Institute of Technology user on 10 April 2019

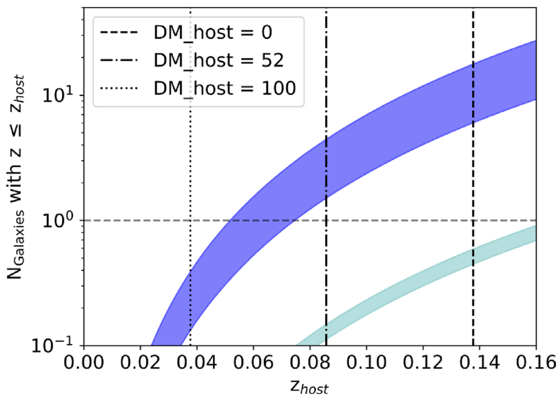

Figure 3. The expected number of galaxies in the FRB 110214 localization area for a range of dwarf galaxy (dark blue), and massive galaxies (cyan) number densities. The horizontal dashed line indicates where a single galaxy is expected. The three vertical lines indicate the host galaxy redshift for a host DM contribution of 0 (dashed), 100 (dotted), and 52 pc cm^{-3} (dot–dashed) which gives the same IGM to host DM ratio as FRB 121102.

5 DISCUSSION AND CONCLUSIONS

FRB 110214 has one of the lowest DMs of the entire FRB sample to-date. The multibeam detection and also the fact that it was only seen in the lower half of the band indicate that the FRB occurred in the MB sidelobes. From our analysis of the best available model of the MB beam pattern we have identified three possible regions on the sky where the burst may have originated at different separations from the centre of the primary beam. From these locations relative to the primary beam we have estimated the intrinsic fluence of the burst in the bottom half of the bandwidth where it would be 50 Jy ms if located in the innermost region, to a maximum of ~2000 Jy ms if located in the outermost. Even in the most conservative case, this would make FRB 110214 one of the highest fluence FRBs detected with Parkes. Despite the high implied brightness, the required energetics to produce the burst are still consistent with those of other known FRBs due to the very low inferred distance. Assuming the burst originated at the maximum estimated redshift of $z = 0.14$ the total isotropic energy required would be $E_{\rm FRB,\,iso} = 3.7-135 \times 10^{32}$ J ($\times 10^{39}$ erg) for the entire range of estimated fluences in Table 3. Even at the high end of this range, the implied energy is still lower than that of FRB 160102 with $E_{160102,\,\rm iso} = 628 \times 10^{32}$ J if it originated at its maximum implied redshift $z = 2.1$.

Not all the localization regions identified for FRB 110214 are equally likely if FRBs are isotropically distributed with a steep brightness distribution. Assuming a Euclidean distribution with a $\log N$–$\log S$ slope of $\alpha = -1.5$, regions where the peak flux density of FRB 110214 is lower are more probable. Based on this assumption, we calculate a fractional likelihood for all locations in each region relative to the minimum peak flux density of 17.7 Jy, which occurs in Region A. For example, considering all locations with a fractional likelihood $(S_i/S_{\rm min})^{-1.5} \geq 0.10$ or 10 per cent results in the exclusion of 90 per cent of Region C and 54 per cent of Region B. All of the locations in Region A are above this threshold. These more limited probability regions contours are shown in Fig. 2 in yellow.

However, the true flux distribution of FRBs remains unknown. A shallower distribution of $\alpha = -0.6$ has been suggested by Vedantham et al. (2016) and early results from ASKAP suggest a steeper than Euclidean distribution of $\alpha = -2.1^{+0.6}_{-0.5}$ (Shannon et al. 2018). The latter case would further favour Region A. A larger statistical sample is needed, however, to determine the true value.

An ultrabright FRB originating in one of the outer regions is still possible, but in either case an origin closer to the detection beam is more likely. Despite significant follow-up efforts with the Parkes telescope, FRB 110214 has not been seen to repeat; most follow-up presented here was focused on searches in Region A. The low DM (and thus small implied distance) and the high intrinsic fluence make this source an excellent candidate for further follow-up. A sensitive telescope such as Parkes or MeerKAT centred on or near the true sky position should be able to detect fainter repeating pulses, even if the source pulse energy distribution were steep. In our monitoring observations, no pulses were detected above a flux density of 0.15 Jy in almost 100 h of follow-up.

There was a bright galaxy in the innermost localization region of FRB 110214, the elliptical galaxy FRL 692 at $z \simeq 0.025$. This is a similar case to the lowest DM FRB of the ASKAP sample, FRB 171020 which was found to have one bright and potentially interesting field galaxy in the error region, ESO 601−G036 (Mahony et al. 2018). The error region for FRB 171020 (0.38 deg^2) was much larger than that of FRB 110214 (0.014 deg^2) and thus the large positional uncertainty made it similarly difficult to precisely identify a host. Ultimately, more precise localization can only be achieved through the detection of repeating pulses.

If FRB 110214 is found to repeat and can be localized through its single pulses it could provide us with one of the closest FRB host galaxies available for study. A host galaxy in the local Universe, particularly if FRB 110214 is found to reside in a dwarf galaxy like FRB 121102, would provide a rich opportunity to study the structure and composition of the host that have been limited for FRB 121102 due to low-signal to noise and the long integration times necessary to obtain spectra. Thus, although the total available observing time for follow-up of archival FRBs is limited, we argue that FRB 110214 should be one of the top priorities for monitoring campaigns in the future.

The localization regions presented here are not exact, as the MB beam model used is only an approximation. The sky around the regions identified here should also be monitored, such as with a phased array feed on a single dish, or with a number of overlapping or adjacent beams formed on the field with an interferometer. FRB surveys are sensitive to bright bursts over more of the sky, and high fluence events like FRB 110214 will be detectable in the telescope sidelobes. Thus, future surveys with multibeam instruments should take great care to model and understand the beam and sidelobe patterns of their instruments in order to more accurately localize bright bursts on the sky.

ACKNOWLEDGEMENTS

The authors thank the anonymous referee for their comments and feedback which improved the quality of the manuscript. The Parkes radio telescope is part of the Australia Telescope National Facility which is funded by the Commonwealth of Australia for operation as a National Facility managed by CSIRO. Parts of this research were conducted by the Australian Research Council Centre of Excellence for All-sky Astrophysics (CAASTRO), through project number CE110001020 and the ARC Laureate Fellowship project FL150100148. This work was performed on the gSTAR national facility at Swinburne University of Technology. gSTAR is funded by Swinburne and the Australian Government's Education Investment Fund. EP and LCO acknowledge funding from the European Research Council under the European Union's Seventh Framework

Downloaded from https://academic.oup.com/mnras/article-abstract/482/3/3109/5145856 by California Institute of Technology user on 10 April 2019

Programme (FP/2007-2013)/ERC Grant Agreement No. 617199. SBS is supported by NSF award #1458952. BWS acknowledges funding from the European Research Council (ERC) under the European Union's Horizon 2020 research and innovation programme (grant agreement No 694745). This research made use of data obtained from the Chandra Source Catalogue, provided by the Chandra X-ray Center (CXC) as part of the Chandra Data Archive. This research made use of Astropy,[5] a community-developed core Python package for Astronomy (Astropy Collaboration et al. 2013; Price-Whelan et al. 2018).

REFERENCES

Astropy Collaboration, 2013, A&A, 558, A33
Baldry I. K. et al., 2012, MNRAS, 421, 621
Bhandari S. et al., 2018, MNRAS, 475, 1427
Champion D. J. et al., 2016, MNRAS, 460, L30
Chatterjee S. et al., 2017, Nature, 541, 58
Chippendale A. P., Beresford R. J., Deng X., Leach M., Reynolds J. E., Kramer M., Tzioumis T., 2016, International Conference on Electromagnetics in Advanced Applications (ICEAA), Cairns, QLD. p. 909
Connor L., Sievers J., Pen U.-L., 2016, MNRAS, 458, L19
Cordes J. M., Lazio T. J. W., 2002, preprint (arXiv:astro-ph020715)
Cordes J. M., Wasserman I., 2016, MNRAS, 457, 232
Evans I. N. et al., 2010, ApJS, 189, 37
Faber S. M. et al., 2007, ApJ, 665, 265
Fairall A. P., 1984, MNRAS, 210, 69
Falcke H., Rezzolla L., 2014, A&A, 562, A137
Farah W. et al., 2018, MNRAS, 478, 1209
Haynes M. P. et al., 2011, AJ, 142, 170
Ioka K., 2003, ApJ, 598, L79
Keith M. J. et al., 2010, MNRAS, 409, 619
Lorimer D. R., Bailes M., McLaughlin M. A., Narkevic D. J., Crawford F., 2007, Science, 318, 777
Macquart J.-P., Shannon R. M., Bannister K. W., James C. W., Ekers R. D., Bunton J. D., 2018, preprint (arXiv:1810.04353)
Mahony E. K. et al., 2018, ApJ, 867, L10
McMahon R. G., Banerji M., Gonzalez E., Koposov S. E., Bejar V. J., Lodieu N., Rebolo R. VHS Collaboration, 2013, The Messenger, 154, 35
Metzger B. D., Berger E., Margalit B., 2017, ApJ, 841, 14
Michilli D. et al., 2018, Nature, 553, 182
Obrocka M., Stappers B., Wilkinson P., 2015, A&A, 579, A69
Oslowski S. et al., 2018, The Astronomer's Telegram, 11385
Petroff E. et al., 2015, MNRAS, 447, 246
Petroff E. et al., 2016, PASA, 33, e045
Planck Collaboration, 2016, A&A, 594, A13
Price-Whelan A. M. et al., 2018, AJ, 156, 123
Ravi V., 2019, MNRAS, 482, 1966
Ravi V. et al., 2016, Science, 354, 1249
Rosen S. R. et al., 2016, A&A, 590, A1
Shannon R. M. et al., 2018, Nature, 562, 386
Skrutskie M. F. et al., 2006, AJ, 131, 1163
Spitler L. G. et al., 2014, ApJ, 790, 101
Spitler L. G. et al., 2016, Nature, 531, 202
Staveley-Smith L. et al., 1996, Publ. Astron. Soc. Aust., 13, 243
Tendulkar S. P. et al., 2017, ApJ, 834, L7
Thornton D. et al., 2013, Science, 341, 53
Totani T., 2013, PASJ, 65, L12
Vedantham H. K., Ravi V., Hallinan G., Shannon R. M., 2016, ApJ, 830, 75
Xu J., Han J. L., 2015, RAA, 15, 1629
Yao J. M., Manchester R. N., Wang N., 2017, ApJ, 835, 29
York D. G. et al., 2000, AJ, 120, 1579

[5]http://www.astropy.org

SUPPORTING INFORMATION

Supplementary data are available at *MNRAS* online.

region_contours_alpha1.5.con
region_contours.con

Please note: Oxford University Press is not responsible for the content or functionality of any supporting materials supplied by the authors. Any queries (other than missing material) should be directed to the corresponding author for the article.

[1]*Anton Pannekoek Institute for Astronomy, University of Amsterdam, PO Box 94249, NL-1090 GE Amsterdam, the Netherlands*
[2]*ASTRON Netherlands Institute for Radio Astronomy, Oude Hoogeveensedijk 4, NL-7991PD Dwingeloo, the Netherlands*
[3]*Centre for Astrophysics and Supercomputing, Swinburne University of Technology, Mail H30, PO Box 218, VIC 3122, Australia*
[4]*Jodrell Bank Center for Astrophysics, University of Manchester, Alan Turing Building, Oxford Road, Manchester M13 9PL, UK*
[5]*ARC Center of Excellence for All-Sky Astronomy (CAASTRO), Swinburne University of Technology, Mail H30, PO Box 218, VIC 3122, Australia*
[6]*ARC Center of Excellence for Gravitational Wave Discovery (OzGrav), Swinburne University of Technology, Mail H11, PO Box 218, VIC 3122, Australia*
[7]*Max-Planck-Institut für Radioastronomie, Auf dem Hügel 69, D-53121 Bonn, Germany*
[8]*CSIRO Astronomy & Space Science, Australia Telescope National Facility, PO Box 76, Epping, NSW 1710, Australia*
[9]*International Centre for Radio Astronomy Research, Curtin University, Bentley, WA 6102, Australia*
[10]*INAF - Osservatorio Astronomico di Cagliari, Via della Scienza 5, I-09047 Selargius (CA), Italy*
[11]*Department of Physics and Astronomy, West Virginia University, PO Box 6315, Morgantown, WV 26506, USA*
[12]*Center for Gravitational Waves and Cosmology, West Virginia University, Chestnut Ridge Research Building, Morgantown, WV 26505, USA*
[13]*SKA Organisation, Jodrell Bank Observatory, Cheshire SK11 9DL, UK*
[14]*Department of Physics and Astronomy, University of British Columbia, 6224 Agricultural Road, Vancouver, BC V6T 1Z1, Canada*
[15]*Università degli Studi di Cagliari, Dep. of Physics, S.P. Monserrato-Sestu Km 0,700, I-09042 Monserrato, Italy*
[16]*Cahill Center for Astronomy and Astrophysics, MC 249-17, California Institute of Technology, Pasadena, CA 91125, USA*
[17]*Institute for Radio Astronomy & Space Research, Auckland University of Technology, Private Bag 92006, Auckland 1142, New Zealand*

This paper has been typeset from a TEX/LATEX file prepared by the author.

Downloaded from https://academic.oup.com/mnras/article-abstract/482/3/3109/5145856 by California Institute of Technology user on 10 April 2019